Flow Structures in the Bottom Region of Riser

Haiyan Zhu[*]   Jesse Zhu[†]

[*]The University of Western Ontario, hzhu23@uwo.ca

[†]The University of Western Ontario, zhu@uwo.ca

FLOW STRUCTURES IN THE BOTTOM REGION OF RISERS

Haiyan Zhu and Jesse Zhu
Departments of Chemical and Biochemical Engineering,
University of Western Ontario, London, Ontario, N6A 5B9

Abstract

This paper studied hydrodynamic characteristics in bottom region of CFB risers with FCC particles over a wide range of operating conditions. Results included solids concentration, particle velocity, and probability density distributions. Comparisons were made between flow structures in riser bottom region and that in bubbling and turbulent fluidized bed.

Introduction

During the past two decades, circulating fluidized beds (CFBs) have been widely applied in chemical, petrochemical, metallurgical, environmental and energy industries (Berruti *et al*. (1), Dry *et al*. (2)). In order to continuously improve design efficiency and performance of existing industrial processes and present new applications, intensive studies have been conducted to obtain more detailed and reliable fundamental knowledge about CFBs (e.g. Li and Kwauk (3), Rhodes et al. (*4*), Lackermeier *et al*. (5), Yang *et al*. (6)). Although the hydrodynamics of CFBs have been investigated to some extent both in industry and academia, much remains to be known about this special multi-phase system, especially in its bottom dense region.

It is well known that, solids distributions in a CFB vary strongly with axial and radial directions. This non-uniform solids distribution can affect the flow structures in risers, and further affect reaction rates, mass and heat transfer, and erosion within riser reactors (Adánez *et al*. (7)). Previous studies have shown that, axial profiles of solids concentration in a CFB riser can be divided into three regions: a bottom dense region, a upper dilute region, and a transition region between them (Li and Kwauk (3), Rhodes *et al*. (4), and Issangya *et al*. (9)). Operating conditions (Rhodes *et al*. (4)), system structures (Svensson *et al*. (10), solid inventory (Kim *et al*. (11)), particle and gas properties (Xu *et al*. (12)) have been found to influence the solids distributions.

In the upper dilute region of a riser, it is widely accepted that there exists a core-annulus flow structure, with a rapid upflowing dilute core region surrounded by a dense annulus, where solids may travel downwards on average or upwards at a much slower velocity (Rhodes *et al*. (4), Issangya *et al*. (9), Brereton *et al*. (13)). In contrast to the upper dilute region, which has been paid more attention and the flow structure in it is relatively clear now; in literature there is significant controversy on

actual events occurring in the bottom region and what flow regimes can be applied in this region. There are mainly two opinions in literature: 1) bubbling flow regime (Rhodes *et al*. (4), Svensson *et al*. (14), Werther (15)), 2) turbulent flow regime (Bai *et al*. (16)). Although previous studies gave some insight into the flow structures of the dense region in CFB risers, up to now no general agreement has been reached. On the other hand, due to the high solids holdup and the high reactant concentrations, a significant portion of the reaction takes place in this region (Schlichthaerle *et al*., (17), Sternéus *et al*. (18)), therefore the flow structures in the bottom region are critical to the overall hydrodynamic and mixing behaviors in circulating fluidized beds.

In this study, we have undertaken a series of experiments to characterize the flow structures in the bottom dense region of risers. The purpose of this study is to provide new perspective and detailed picture about the flow state in this special region based on measurements of solids concentration and velocity over a wide range of operating conditions.

Experimental systems

The experiments were conducted in a circulating fluidized bed system (10 m in height) shown schematically in Fig.1. Air was introduced into the riser bottoms through perforated distributor plates with 14% opening area. Solids used in all experiments were spent FCC catalyst with a Sauter mean diameter of 65 µm and a particle density of 1780 kg/m^3. Newly developed reflective optical fiber probes were used to measure instantaneous solids concentration and velocity simultaneously. Diameter of the probes is 3.8 mm, containing two sub-probes with a separation distance of 1.7 mm. The sub-probes consist both light-emitting and receiving quartz fibers, arranged in an alternating array, corresponding to emitting and receiving layers of fibers, diameter of the fibers is 25 µm. Cross-correlation methods were used here to calculate particle velocity based on the measurements from two sub-probes. The relationship between the output signals of the optical fiber probe and the solids

Fig.1 Schematic drawing of the circulating fluidized bed

concentration in the measurement volume is non-linear. Therefore, a reliable calibration is necessary to ensure an accurate measurement. Details of the calibration system were described by Zhang et al. (19).
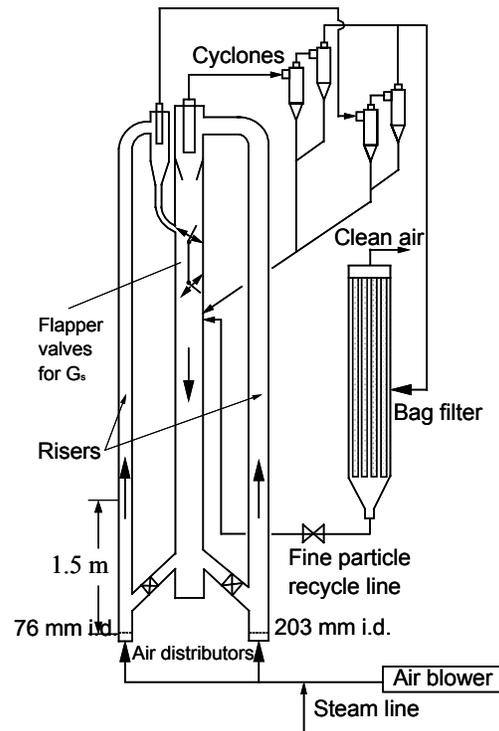
Results and discussion

Measurements were carried out in two risers with different inner diameters, 0.076 and 0.203 m, respectively. At an axial measurement location (*H* = 1.5 m), local solids

volume concentration (ε_s) and velocity (V_s) were measured at eleven radial positions. At each measuring position sampling time was set as 13.1s with a frequency of 50 kHz, and measurements were repeated at least five times. Direction of particle movements was determined based on the maximum cross-correlation coefficient from the forward and backward correlation of the measured signals.

Bottom region with different density

Fig.2 ploted the axial profiles of mean solids concentrations for different solids flow rates and superficial gas velocities obtained from our previous studies (Pärssinen and Zhu (20), Yan and Zhu (21)). The axial voidage profiles clearly provided evidence that the solids concentration was a strong function of height and operating conditions. Depending on the operating conditions, three different axial solids distribution profiles are observed: uniform axial profile with constant solids volume concentration ($\bar{\varepsilon}_s$ < 0.02) throughout the entire riser; exponential profile with continuous decreasing solids holdup until reaching a constant value at the upper section of the riser; and S-shaped profile with a stable dense region at the bottom ($\bar{\varepsilon}_s$ > 0.1) and the dilute region at the top of the riser. The present investigation focuses on the flow structures in a dense bottom region with a cross-sectional averaged solids concentration larger than 0.1.
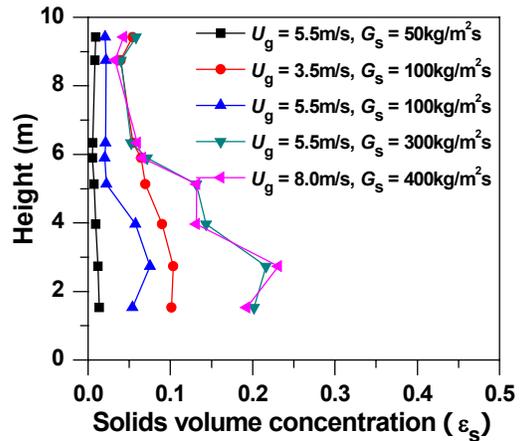
Fig.2 Axial solids holdup distributions in 0.076mm riser (Pärssinen and Zhu (20), Yan and Zhu (21))

Radial solids concentration distribution in bottom region

Fig.3 shows the effects of operating conditions (U_g, G_s) on the radial profiles of time-average solids concentrations. Measurements are taken in the bottom region (H = 1.5 m) of the 0.076 mm-i.d.-riser. Uniform solids volume holdups distribution is found in the center region of the riser (0 < r/R < 0.4) for all operating conditions, and the solids holdup in this region is insensitive to the changes of operating conditions (ε_s= 0.01~0.035). Moreover, for G_s = 50 kg/m²s and U_g = 8.0 m/s, the profile is nearly flat over the whole cross-section, presenting characteristics of the dilute pneumatic transport regime, with overall cross-sectional average solids concentration of about 0.01. However, for region r/R > 0.6, with decreasing U_g or increasing G_s, the solids concentration increases rapidly from the center towards the wall and reaches its maximum value around 0.38 near the wall. It is worth noting that there is no clear boundary between the dilute central region and the dense wall region, and the transition between them was a gradual process.

The results from these five operating conditions show that, in the bottom region of the riser, the profiles of solids concentrations are non-uniform and such non-uniformity increases with G_s, and decreases with U_g. The significant difference in solids concentration mainly happens in the region r/R > 0.6, suggesting that U_g and G_s have greater influences on the wall region than on the core region.

This non-uniform solids distribution is clearly different than that in a bubbling fluidized bed, where a rather uniform average radial solids distribution profiles has been found (Andreux *et al*. (22)).

Corresponding cross-sectional average solids concentrations for the above operation conditions at H = 1.5 m are summarized in Table 1. Combining with the axial solids concentration profiles (Fig.2), one can conclude that the appearance of core-annulus flow structure in the bottom region is corresponding to the establishment of the S-shape axial solids concentration profile with cross-sectional average solids concentration larger than 0.1 at the bottom section.
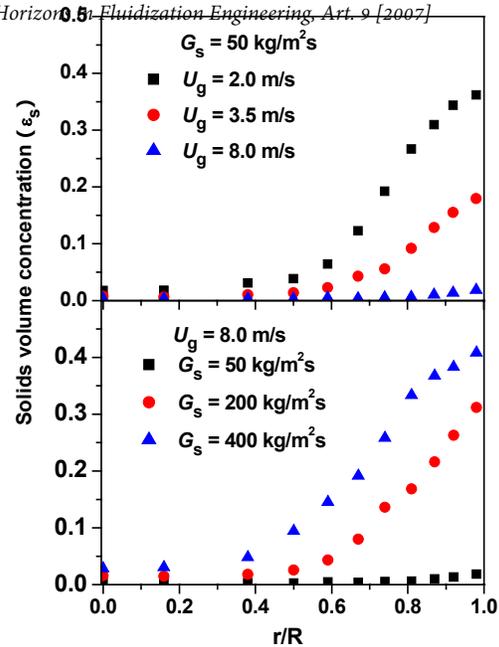
Fig.3 Effects of operation conditions on radial solids concentration (H = 1.5 m)

Table 1

	U_g = 2.0 m/s	U_g = 3.5 m/s	U_g = 8.0 m/s	U_g = 8.0 m/s	U_g = 8.0 m/s
	G_s= 50kg/m^{2}s	G_s=50kg/m^{2}s	G_s=50kg/m^{2}s	G_s=200kg/m^{2}s	G_s=400kg/m^{2}s
$\overline{\varepsilon}_s$	0.161	0.085	0.006	0.101	0.203

Radial particle velocity profiles in bottom region

Upflowing ($V_{p,vp}$) and downflowing ($V_{p,down}$) particle velocity variations with U_g and G_s at the bottom region of CFB are plotted in Fig.4. Generally, in the bottom zone, the largest $V_{p,vp}$ always appears at the central region. Moving outwards towards the wall, $V_{p,vp}$ significantly decreases. With increasing U_g, $V_{p,vp}$ increases; and the velocity profile becomes flatter. However, $V_{p,vp}$ changes a little at the wall. $V_{p,vp}$ decreases with increasing G_s, and the radial velocity profile becomes steeper. Fig.4 also shows that at low U_g (2.0 and 3.5 m/s), the highest $V_{p,down}$ appears at a middle region of the riser, instead of the wall region. It is worth noting that under high flux condition (G_s = 200 and 400 kg/m^{2}s), $V_{p,down}$ is less sensitive to the changes of G_s.
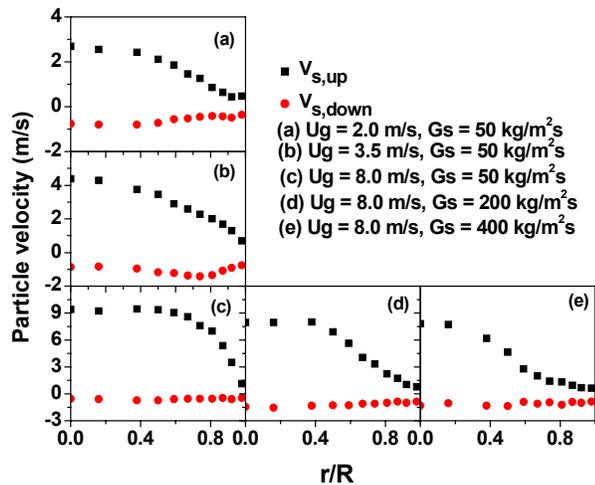
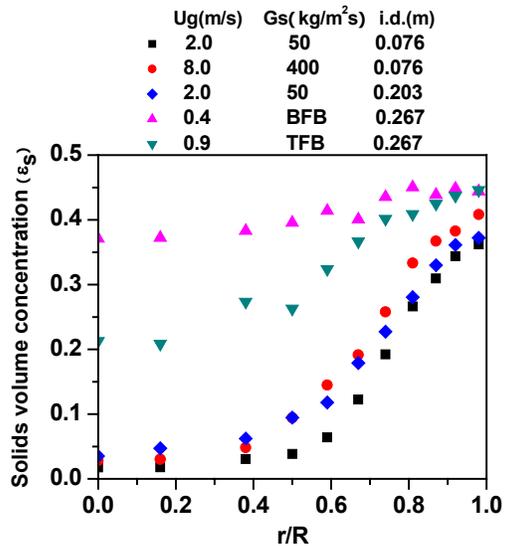**Fig.4 Particle velocity profiles in 0.076mm riser under various operation conditions**

Comparison with turbulent fluidized bed

Although in the literature some researchers have treated the bottom dense region in a CFB riser as bubbling or turbulent fluidized bed, there is no comprehensive comparison and a solid proof to support their claims. In this study, a comparison of the radial solids concentration profiles in the bottom region of CFBs and TFB is carried out, as shown in Fig.5. Measurements of solids concentration in TFB are taken with the same optical fiber probe as used in the risers. All the solids concentration profiles show an evolution to increased solids concentration with increasing radial distance, with greater evolution in the riser and the least for the TFB case. Fig.5 also shows a clear relationship between the column diameter and the average cross-sectional solids concentration. Under the same operation conditions, the larger bed is much denser than the smaller one. However, there are no significant changes in the general shape of the profiles, which have a flat central region and a dense annulus region with the solids holdup increasing sharply toward the wall.

To compare the dynamic gas-solids distributions in the riser and in the bubbling and turbulent fluidized beds, probability density distributions of measured transient solids holdup signals are examined at different radial positions, as illustrated in Fig.6. Depending on the operating conditions and the spatial locations, single- or two-peak PDD profiles are found. Two-peak plots represent the coexistence of the dilute and the dense phases, and single-peak plots indicate the flow is dominated by just one phase (Zhang et al. (23)). Therefore, a flatter and wider distributed PDD suggests a better mixed flow state. Generally, it could be seen that decreasing U_g or increasing G_s leads to a decrease of the probability density in the dilute phase and increase of the probability density in the dense phase.

Ug(m/s)	Gs(kg/m^{2}s)	i.d.(m)
2.0	50	0.076
8.0	400	0.076
2.0	50	0.203
0.4	BFB	0.267
0.9	TFB	0.267

Fig.5 Comparison of radial solids concentration distribution in riser bottom region and TFB

A longer tail on the right hand side of dilute phase peak and left hand side of the dense phase peak are also observed at high flux flow conditions ($G_s \geq 200$ kg/m^{2}s)

When combining the evolution of PDD across the whole section of the column with the corresponding cross-sectional average solids concentration ($\bar{\varepsilon}_s$), it can be found that for $\bar{\varepsilon}_s \leq 0.1$, the PDD curves show a single dilute phase peak distribution at all radial positions with the peaks at solids concentration of less than 0.02, which is similar with the probability distribution for dilute transport flow regime. However, when $\bar{\varepsilon}_s$ increases beyond 0.1, two different PDDs are observed at different radial positions: for the region $r/R < 0.5$, the PDD curves still keep the single-peak distribution as that in the dilute transport flow; but when moving outwards towards the wall, the PDDs exhibit two-peak model with a continuous solids concentration. Comparing the above PDD models in the bottom of the risers with that in the

bubbling fluidized bed, where there is a clearly pure two-phase flow structure, which represents by two-peak PDD with no singles for the solids concentration between 0.1~0.4, it can be concluded that the bubbling flow regime cannot be applied to the bottom region of riser. Moreover, the similar two-peak and wide distribution PDD curves happening at the region r/R > 0.5 in the risers for the cases of $\bar{\varepsilon}_s$ > 0.1 and r/R < 0.67 in TFB suggest the similarity in gas-solid flow structures in these two regions.

The above analysis and comparison show that it is insufficient to simply treat the whole bottom dense region in the riser as one current existing flow regime, such as bubbling or turbulent flow regime. Depending on the cross-sectional solids concentration values, there are two different flow structures in the bottom region of the riser. For $\bar{\varepsilon}_s$ ≤ 0.1, corresponding to the non-S-shaped axial solids distribution, the flow structures in the bottom region may be treated as the dilute transport. When $\bar{\varepsilon}_s$ > 0.1, where a S-shaped axial solids distribution appearing, the characterization of fluidization shows a gradual transition from dilute transport flow regime to turbulent flow regime. Fig.6 further demonstrates that the gas-solid distribution is different even when there is little or no difference in the local solids concentration, as shown by the marked difference among PDDs in the wall regions of the risers and the turbulent fluidized bed.

Conclusions

The study seeks to improve the understanding of the complex hydrodynamic behavior in the bottom region of CFB riser with FCC particles. The results included radial solids concentration, particle velocity profiles, and probability density distributions. For all operating conditions investigated, the solids concentration remains low and relatively constant in the central region of the risers. With increasing the solids circulation rate, G_s, and/or decreasing the superficial gas velocity, U_g, significant increases in the solids concentration happen in the region *r/R* > 0.5. At the same operating conditions, the larger riser is much denser than the smaller one, although their trends of radial solids distribution profiles are similar. The probability density distribution analysis show that under the operating conditions where non-S-shaped axial solids concentration profile exists, the flow structures in the bottom region belong to the dilute transport flow regime. And for the S-shaped axial solids distribution cases or for the cross-sectional average solids concentration higher than 0.1 conditions, the radial solids concentration profiles show a dilute core region surrounded by a dense-annular zone in the bottom dense region. The characterization of fluidization shows a gradual transition from the dilute transport flow regime to the turbulent flow regime. Moreover, in the core region, the local time mean solids concentration is low, and non-sensitive to the changes of operating conditions. This conclusion is based on the experiments with limited range of riser diameter and operating conditions, further investigation needs to be done in other fluidization systems (e.g., larger column diameter) under conditions operating where the axial S-shaped solids concentration profile or the cross-sectional average solids concentration larger than 0.1 condition is observed. The particle velocity results show that the solids upflowing velocity is always larger than the downflowing velocity at all radial positions, indicating that the flow of particles in the bottom region is predominantly upward through the whole cross section of the risers. And the

superficial gas velocity has great influence on the solids downflowing velocity than the solids flow rate. Under high solids flux conditions (Gs > 200 kg/m^{2}s), the solids downflowing velocity is not sensitive to both radial positions and solids flow rates.
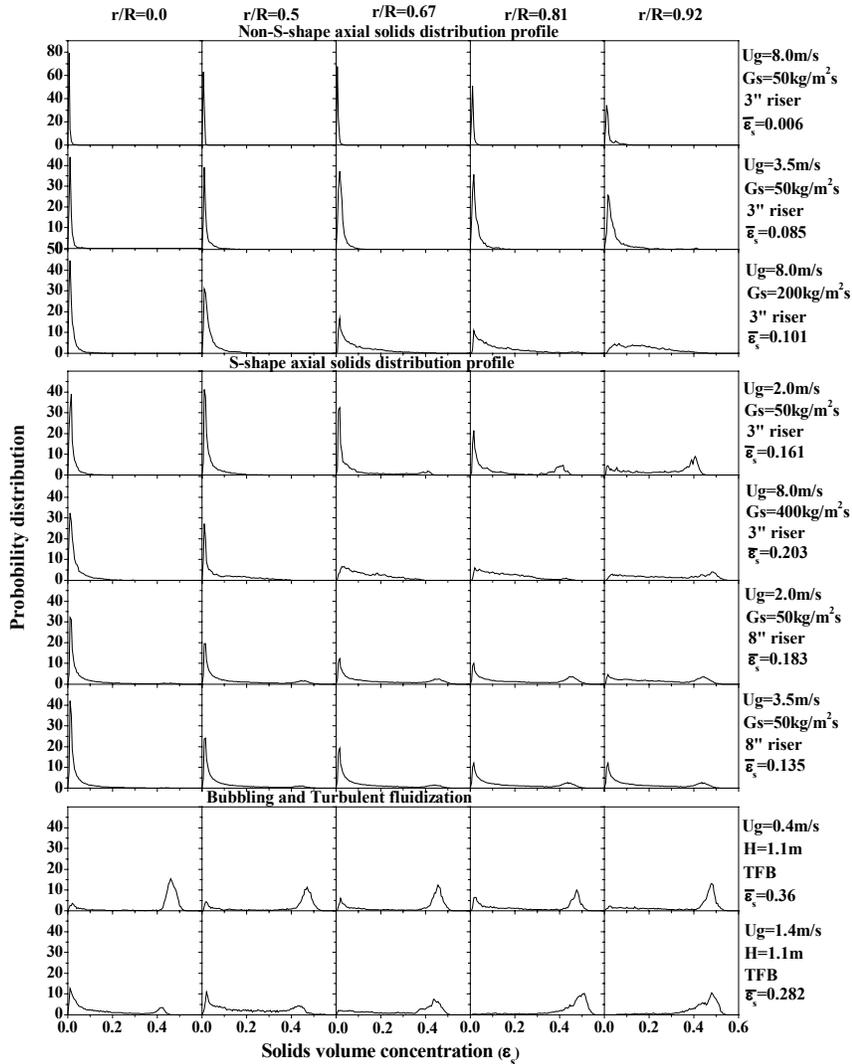

Fig.6 Comparison between the probability density distribution of local solids concentration in bottom region of CFB and TFB

Reference

1. Berruti, F., Chaouki, J., Godfroy, L., Pugsley, T. S., Patience, G. S. 1995, Hydrodynamics of circulating fluidized red risers: A review, Canadian Journal of Chemical Engineering, 73, 579-602
2. Dry, R., Beeby, C. J. 1997, Applications of CFB technology to gas-solid reactions, In Grace, J.R., Avidan, A.A., Knowlton, T.M., Circulating fluidized beds, 441-465
3. Li, Y., Kwauk, M. 1980, The dynamics of fast fluidization, In Grace, J.R., Matsen, J.M, Fluidization, 537-544
4. Rhodes, M.J., Sollaart, M., Wang, X.S. 1998, Flow structure in a fast fluidized bed, Powder Technology, 99, 194-200

5. Lackermeier, U., Rudnick, C., Werther, J., Bredebusch, A., Burkhardt, H. 2001, Visualization of flow structures inside a circulating fluidized bed by means of laser sheet and image processing, Powder Technology, 114, 71-83

6. Yang, N., Wang, W., Ge, W., Li J.H. 2003, CFD simulation of concurrent-up gas–solid flow in circulating fluidized beds with structure-dependent drag coefficient, Chemical Engineering Journal, 96, 71-80

7. Adánez, J., Gayán, P., García-Labiano, F., de Diego, L.F. 1994, Axial voidage profiles in fast fluidized beds, Powder Technology, 81, 259-268

8. Bai, D., Shibuya, E., Masuda, Y., Nishio, K., Nakagawa, N., Kato, K. 1995, Distinction between upward and downward flows in circulating fluidized beds, Powder Technology, 84, 75-81

9. Issangya, A.S., Bai, D., Bi, H.T., Lim, K.S., Zhu, J., Grace J.R. 1999, Suspension densities in a high-density circulating fluidized bed riser, Chemical Engineering Science, 54, 5451-5460

10. Svensson, A., Johnsson, F., Leckner, B. 1996, Fluidization regimes in non-slugging fluidized beds: the influence of pressure drop across the air distributor, Powder Technology, 86, 299-312

11. Kim, S.W., Kirbas, G., Bi, H.T., Lim, C.J., Grace, J.R. 2004, Flow behavior and regime transition in a high-density circulating fluidized bed riser, Chemical Engineering Science, 59, 3955-3963

12. Xu, G.W., Nomura, K., Nakagawa, N., Kato, K. 2000, Hydrodynamic dependence on riser diameter for different particles in circulating fluidized beds, Powder Technology, 113, 80-87

13. Brereton, C.M.H., Grace, J.R. 1993, Microstructural aspects of the behavior of circulating fluidized beds, 48, 2565-2572

14. Svensson, A., Johnsson, F., Leckner, B. 1996, Bottom bed regimes in a circulating fluidized bed boiler, Inr. J. Multiphase Flow, 22, 1187-1204

15. Werther, J. 1994, Fluid mechanics of large-scale CFB units, In Avidan, A.A., Circulating fluidized bed technology IV, 1-14, New York

16. Bai, D., Shibuya, E., Masuda, Y., Nakagawa, N., Kato, K. 1995, Flow structure in a fast fluidized bed, Chemical Engineering Science, 51, 957-966

17. Schlichthaerle, P., Werther, J. 1999, Axial pressure profiles and solids concentration distributions in the CFB bottom zone, In: Werther, J., Circulating fluidized bed technology VI, 185-190

18. Sternéus, J., Johnsson, F., Leckner, B., Palchonok, G.I. 1999, Gas and solids flow in circulating fluidized beds - discussion on turbulence, Chemical Engineering Science, 54, 5377-5382

19. Zhang, H., Johnston, P.M., Zhu, J. X., de Lasa, H.I., Bergougnou, M.A. 1998, A novel calibration procedure for a fiber optic solids concentration probe, Powder Technology, 100, 260-272

20. Pärssinen, J.H., Zhu, J.X. 2001, Axial and radial solids distribution in a long and high-flux CFB riser, AIChE Journal, 47, 2197-2205

21. Yan, A.J., Zhu, J.X. 2004, Scale-up effect of riser reactors (1): Axial and radial solids concentration distribution and flow development, Ind. Eng. Chem. Res., 43, 5810-5819

22. Andreux, R., Gauthier, T., Chaouki, J., Simonin, O. 2005, New description of fluidization regimes, AIChE Journal, 51, 1125-1130

23. Zhang, M.H., Qian, Z., Yu, H., Wei, F. 2003, The solid flow structure in a circulating fluidized bed riser/downer of 0.42-m diameter, Powder Technology, 129, 46-52